A modified Al_2O_3 coating process to enhance the electrochemical performance of $Li(Ni_{1/3}Co_{1/3}Mn_{1/3})O_2$ and its comparison with traditional Al_2O_3 coating process

Youyuan Huang, Jitao Chen, Fuquan Cheng, Wang Wan, Wen Liu, Henghui Zhou[*], Xinxiang Zhang

College of Chemistry and Molecular Engineering, Peking University, Chengfu Road 202, Haidian District, Beijing 100871, PR China

ABSTRACT

Al_2O_3-modified $Li(Ni_{1/3}Co_{1/3}Mn_{1/3})O_2$ is synthesized by a modified Al_2O_3 coating process. The Al_2O_3 coating is carried out on an intermediate, $(Ni_{1/3}Co_{1/3}Mn_{1/3})(OH)_2$, rather than on $Li(Ni_{1/3}Co_{1/3}Mn_{1/3})O_2$. As a comparison, Al_2O_3-coated $Li(Ni_{1/3}Co_{1/3}Mn_{1/3})O_2$ also is prepared by traditional Al_2O_3 coating process. The effects of Al_2O_3 coating and Al_2O_3 modification on structure and electrochemical performance are investigated and compared. Electrochemical tests indicate that cycle performance and rate capability of $Li(Ni_{1/3}Co_{1/3}Mn_{1/3})O_2$ are enhanced by Al_2O_3 modification without capacity loss. Al_2O_3 coating can also enhance the cycle performance but cause evident capacity loss and decline of rate capability. The effect of Al_2O_3 coating and Al_2O_3 modification on kinetics of lithium-ion transfer reaction at the interface of electrode/electrolyte is investigated via electrochemical impedance spectra (EIS). The result support that the Al_2O_3 modification increase Li^+ diffused coefficient and decrease the activation energy of Li^+ transfer reaction but the traditional Al_2O_3 coating lead to depression of Li^+ diffused coefficient and increase of activation energy.

1. Introduction

Lithium-ion batteries have widely been used as the power source for portable electronic devices and show great prospect in application of HEV and EV [1,2]. Unfortunately, conventional cathode material, $LiCoO_2$, cannot be applied in the large scale lithium-ion batteries for HEV&EV application due to cost and safety issues. More and more attention has been paid to those cathode materials which are lower cost and safer than $LiCoO_2$ [3–6]. $Li(Ni_{1/3}Co_{1/3}Mn_{1/3})O_2$ has been considered a promising alternative to conventional $LiCoO_2$ cathode for lithium-ion batteries due to lower cost, high available capacity and superior safety [7]. Compared with $LiCoO_2$, $Li(Ni_{1/3}Co_{1/3}Mn_{1/3})O_2$ has a stable structure. There is no structural degradation even though $Li(Ni_{1/3}Co_{1/3}Mn_{1/3})O_2$ is charged to 4.6 V, in which it can deliver a capacity of approximate 200 mAh g^{-1} [8]. However, when it is charged to 4.5 V or higher, $Li(Ni_{1/3}Co_{1/3}Mn_{1/3})O_2$ shows appreciable capacity fade during cycling [9,10]. Recent reports indicated that coating with inert metal oxides, such as Al_2O_3, TiO_2, ZrO_2, etc., was effective for enhancing the cycle perfor-

mance of $Li(Ni_{1/3}Co_{1/3}Mn_{1/3})O_2$ at a high charge cut-off voltage [11–13]. The inert metal oxide coating layer on the surface of $Li(Ni_{1/3}Co_{1/3}Mn_{1/3})O_2$ can enhance stability of the interphase and decrease the deleterious reaction between the electrode and electrolyte. Nevertheless, the inert metal oxide coating layer may cause capacity loss and decline of rate capability because of its poor electronic and ionic conductivity. Therefore, some Li-contained oxides, such as $LiAlO_2$ [14,15], were employed to enhance electrochemical performance of $Li(Ni_{1/3}Co_{1/3}Mn_{1/3})O_2$. Compared with inert metal oxide coating layer, the Li-contained oxide coating layer has high Li^+ conductivity and can provide the tunnel for Li^+ transportation during charging and discharging processes. In addition, modifying traditional coating process also is a good choice to improve the performance of $Li(Ni_{1/3}Co_{1/3}Mn_{1/3})O_2$. Recently, we reported a modified ZrO_2 coating process to enhance cycle performance and rate capability of $Li(Ni_{1/3}Co_{1/3}Mn_{1/3})O_2$ [16]. In the process, ZrO_2 coating was carried out on the intermediate, $(Ni_{1/3}Co_{1/3}Mn_{1/3})(OH)_2$, instead of $Li(Ni_{1/3}Co_{1/3}Mn_{1/3})O_2$. One part of the Zr covered the surface of $Li(Ni_{1/3}Co_{1/3}Mn_{1/3})O_2$ as a Li_2ZrO_3 coating layer, and the other part of the Zr diffused into the crystal lattice of $Li(Ni_{1/3}Co_{1/3}Mn_{1/3})O_2$. The special Zr element distribution contribute to improvement of electrochemical performance of $Li(Ni_{1/3}Co_{1/3}Mn_{1/3})O_2$. However, it is still not clear that what will happen if we use other metal oxide instead of ZrO_2 in the modified coating process. Therefore, in this paper, we investigate the effect of the modified Al_2O_3 coating process on electrochemical performance of $Li(Ni_{1/3}Co_{1/3}Mn_{1/3})O_2$.

[*] Corresponding author. Tel.: +86 10 62757908; fax: +86 10 62757908.
E-mail addresses: youyuanh@pku.edu.cn (Y. Huang), chenjitao@pku.edu.cn (J. Chen), fqcheng@pku.edu.cn (F. Cheng), wwbj2008@163.com (W. Wan), liuwen-03721@163.com (W. Liu), hhzhou@pku.edu.cn (H. Zhou), zxx@pku.edu.cn (X. Zhang).

转载

In the modified Al_2O_3 coating process, Al_2O_3 is coated on $(Ni_{1/3}Co_{1/3}Mn_{1/3})(OH)_2$ first, instead of $Li(Ni_{1/3}Co_{1/3}Mn_{1/3})O_2$. Al_2O_3-modified $Li(Ni_{1/3}Co_{1/3}Mn_{1/3})O_2$ is synthesized by sintering the mixture of Al_2O_3-coated $(Ni_{1/3}Co_{1/3}Mn_{1/3})(OH)_2$ and Li_2CO_3. As a comparison, Al_2O_3-coated $Li(Ni_{1/3}Co_{1/3}Mn_{1/3})O_2$ is synthesized by traditional Al_2O_3 coating process. The structure, surface character and electrochemical performance of Al_2O_3-modified $Li(Ni_{1/3}Co_{1/3}Mn_{1/3})O_2$ are investigated. The difference between Al_2O_3-modified $Li(Ni_{1/3}Co_{1/3}Mn_{1/3})O_2$ and Al_2O_3-coated $Li(Ni_{1/3}Co_{1/3}Mn_{1/3})O_2$ is also discussed.

2. Experimental

2.1. Synthesis of Al_2O_3-modified $Li(Ni_{1/3}Co_{1/3}Mn_{1/3})O_2$

Sphere $(Ni_{1/3}Co_{1/3}Mn_{1/3})(OH)_2$ with 8–10 μm diameter was prepared first based on Ref. [16]. To coat $(Ni_{1/3}Co_{1/3}Mn_{1/3})(OH)_2$ with Al_2O_3, $Al(NO_3)_3$ was first dissolved in ethanol at room temperature. The $(Ni_{1/3}Co_{1/3}Mn_{1/3})(OH)_2$ powder was poured into the solution with continuous stirring for 1 h, and then $NH_3 \cdot H_2O$ (2%) was slowly added into the solution and pH was controlled at 8. This mixture was kept at 80 °C for 5 h until most of the solvent was evaporated. The powder was dried at 120 °C for 12 h to obtain the precursor of Al_2O_3-coated $(Ni_{1/3}Co_{1/3}Mn_{1/3})(OH)_2$. The Al content was set at molar ratios of $Al/(Ni+Co+Mn)$ = 0%, 0.5%, 1%, 2%, 5% by controlling the amount of $Al(NO_3)_3$. To prepare Al_2O_3-modified $Li(Ni_{1/3}Co_{1/3}Mn_{1/3})O_2$ powder, stoichiometric amounts of the as-prepared Al_2O_3-coated $(Ni_{1/3}Co_{1/3}Mn_{1/3})(OH)_2$ and Li_2CO_3 were mixed and calcined at 900 °C for 24 h.

As a comparison, Al_2O_3-coated $Li(Ni_{1/3}Co_{1/3}Mn_{1/3})O_2$ was prepared via traditional Al_2O_3 coating process. The $Li(Ni_{1/3}Co_{1/3}Mn_{1/3})O_2$ powder was poured into the $Al(NO_3)_3$ solution with continuous stirring for 1 h, and then $NH_3 \cdot H_2O$ (2%) was slowly added into the solution and pH was controlled at 8. This mixture was kept at 80 °C for 5 h until most of the solvent was evaporated. The powder was dried at 120 °C for 12 h and then was sintered at 500 °C for 6 h.

2.2. Characterization of the structure and physical parameters

X-ray diffractometry (XRD, Rigaku Rint 2200) was employed to characterize the crystal structure of powder sample. XRD data were obtained with Cu Kα radiation (λ = 0.15406 nm) in the 2θ range of 10–80° at a continuous scan mode with a step size of 0.02° and a scan rate of 2° per minute. The particle shape and morphology images of $Li(Ni_{1/3}Co_{1/3}Mn_{1/3})O_2$ were observed with a scanning electron microscope (SEM, Hitachi S-3500N). Energy dispersive X-ray spectroscopy (EDS, Oxford INCA) was employed to analyze the composition and spatial distribution of transition metal elements on the surfaces of materials. The tap density of materials was measured using a tap density tester (FTZ-4, 300 times per minute for 3000 taps). ICP-AES (IRIS Intrepid II, USA) was employed to measure the transition metal element content of materials. X-ray photoelectron spectroscopy (XPS, Kratos Axis Ultra spectrometer with Al Kα radiation, $h\upsilon$ = 1486.71 eV) measurements were performed to investigate information on the surface of materials. Macro-mode (about 4 mm × 4 mm) Ar-ion etching was employed to assist XPS in measuring the concentrations of Al element at different depths from the surface into the bulk of the Al_2O_3-coated and Al_2O_3-modified $Li(Ni_{1/3}Co_{1/3}Mn_{1/3})O_2$. The etching rate was estimated as 0.5 nm per minute for a silica patch.

2.3. Electrochemical measurements

The electrode was fabricated from a 88:7:5 (mass%) mixture of active material: super-P carbon black: polyvinylidene difluo-ride (PVDF). The PVDF was dissolved in *N*-methylpyrrolidinone (NMP), and then the active material and Super-P carbon black were added. After homogenization, the slurry was evacuated for 20 min to remove residual air. The slurry was coated on a thin aluminum foil (20 μm thick) and dried overnight at 120 °C in a vacuum oven. The electrode was pressed at a pressure of 10–20 MPa and punched into round disks with 10 mm diameter. The thickness of the cathode film was about 50 μm. Standard 2032 coin cells were assembled in a dry Ar-filled glove box to test the electrochemical properties of the cathode material. Lithium metal foil was used as the counter electrode and 1.0 mol L^{-1} $LiPF_6$/(EC:EMC:DEC = 1:1:1) as the electrolyte. After aging for 10 h to ensure full wetting of the electrolyte, the cell was charged and discharged for three cycles at a current density of 0.2 C (150 mA g^{-1} was assumed to be the 1 C rate) in the range of 4.3–3.0 V (vs. Li$^+$/Li) for activation. The rate capability was measured by charging the cells to 4.3 V at 0.2 C current and then discharging at current densities of 0.2 C, 0.5 C, 1.0 C, 2.0 C, 3.0 C, and 5.0 C. The electrochemical impedance spectroscopy (EIS) of the coin cell was measured in the frequency range from 0.01 Hz to 100 kHz at a CHI660B electrochemistry work station.

3. Results and discussion

3.1. Morphology and physical property of Al_2O_3-modified $Li(Ni_{1/3}Co_{1/3}Mn_{1/3})O_2$

In order to investigate the effect of Al_2O_3 modification on physical property of $Li(Ni_{1/3}Co_{1/3}Mn_{1/3})O_2$, tap density (TD) and special surface area (SSA) of all samples were measured. These results are given in Table 1. Bare $(Ni_{1/3}Co_{1/3}Mn_{1/3})(OH)_2$ showed a special surface area of 10.59 m^2 g^{-1}. Surface of $(Ni_{1/3}Co_{1/3}Mn_{1/3})(OH)_2$ became coarse after Al_2O_3 coating and the SSA of Al_2O_3-coated $(Ni_{1/3}Co_{1/3}Mn_{1/3})(OH)_2$ gradually increased as Al content increase to 5%. Bare $Li(Ni_{1/3}Co_{1/3}Mn_{1/3})O_2$ showed a special surface area of 0.42 m^2 g^{-1} and a tap density of 2.48 g cm^{-3}. Although SSA of Al_2O_3-coated $(Ni_{1/3}Co_{1/3}Mn_{1/3})(OH)_2$ was larger than that of bare one, all Al_2O_3-modified $Li(Ni_{1/3}Co_{1/3}Mn_{1/3})O_2$ samples show similar SSA and TD to bare sample. The SSA of Al_2O_3-modified $Li(Ni_{1/3}Co_{1/3}Mn_{1/3})O_2$ do not change evidently as Al content increases. On the contrary, 1% Al_2O_3-coated $Li(Ni_{1/3}Co_{1/3}Mn_{1/3})O_2$ showed a SSA of 1.08 m^2 g^{-1} and a TD of 2.34 g cm^{-3}. The SSA increase and TD decrease of $Li(Ni_{1/3}Co_{1/3}Mn_{1/3})O_2$ are caused by traditional Al_2O_3 coating process. The large SSA and low TD of cathode materials are adverse to fabrication of electrode for lithium-ion batteries. ICP–AES was employed to measure Al content of all samples. The results (not shown) indicate that the ratio of $Al/(Ni+Co+Mn)$ is in good agreement with the initial ratio in the mixture.

SEM images of all samples are given in Fig. 1. No significant difference between the bare and 1% Al_2O_3-modified $Li(Ni_{1/3}Co_{1/3}Mn_{1/3})O_2$ was observed by SEM. In contrast, Al_2O_3 coating layer could be observed on the surface of 1% Al_2O_3-coated $Li(Ni_{1/3}Co_{1/3}Mn_{1/3})O_2$ by SEM in Fig. 1(C). The composition and distribution of elements of 1% Al_2O_3-modified $Li(Ni_{1/3}Co_{1/3}Mn_{1/3})O_2$

Table 1
Physical parameter of bare 2, Al_2O_3-modified, Al_2O_3-coated $Li(Ni_{1/3}Co_{1/3}Mn_{1/3})O_2$ and corresponding $(Ni_{1/3}Co_{1/3}Mn_{1/3})(OH)_2$ precursor.

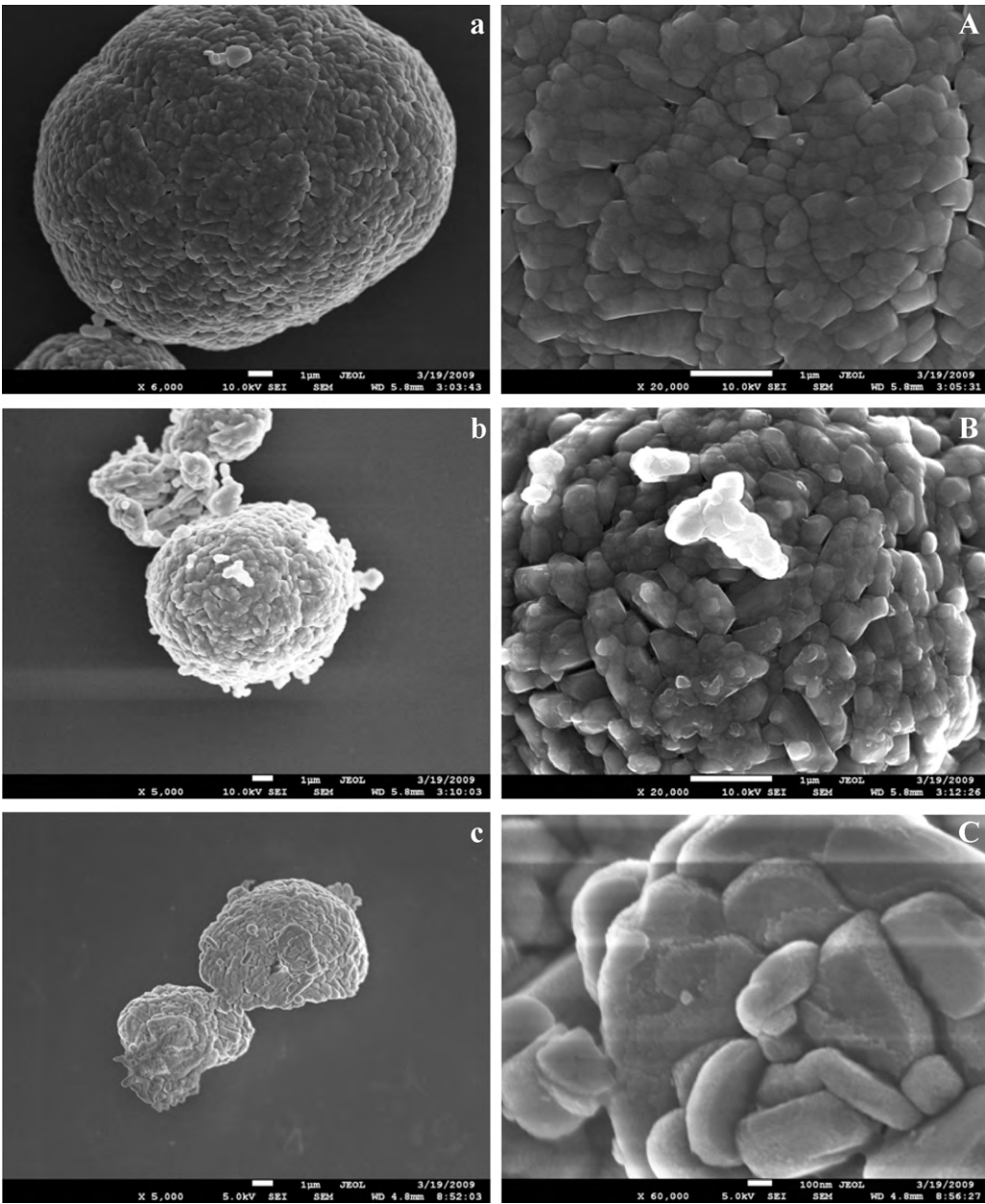| Sample	TD (g cm^{-3})	SSA (m^2 g^{-1})	SSA of $(Ni_{1/3}Co_{1/3}Mn_{1/3})$ $(OH)_2$ (m^2 g^{-1})
Bare	2.48	0.42	10.59
0.5% Al_2O_3-modified	2.47	0.42	13.76
1% Al_2O_3-modified	2.48	0.44	20.79
2% Al_2O_3-modified	2.49	0.45	23.87
5% Al_2O_3-modified	2.47	0.44	28.87
1% Al_2O_3-coated	2.34	1.08	–

Fig. 1. SEM images of bare (a, A), 1% Al_2O_3-modified $Li(Ni_{1/3}Co_{1/3}Mn_{1/3})O_2$ (b, B) and 1% Al_2O_3-coated $Li(Ni_{1/3}Co_{1/3}Mn_{1/3})O_2$ (c, C). A–C are corresponding magnified SEM images of a–c, respectively.

were measured by EDS. As shown in Fig. 2, Al is distributed uniformly on the surface of particles of 1% Al_2O_3-modified $Li(Ni_{1/3}Co_{1/3}Mn_{1/3})O_2$. The further discussion on the surface configuration and distribution of Al along the radial direction of particles will be discussed in later section.

3.2. Effect of Al_2O_3 modification on crystal structure of $Li(Ni_{1/3}Co_{1/3}Mn_{1/3})O_2$

In order to study the effect of Al_2O_3 modification and Al_2O_3 coating on crystal structure of $Li(Ni_{1/3}Co_{1/3}Mn_{1/3})O_2$, crystal structures of all samples were investigated by XRD. As shown in Fig. 3, diffraction patterns of all samples can be identified as a layered α-NaFeO$_2$ structure with space group R-3m and distinct splitting of the [(108), (110)] and [(006), (102)] peaks is observed. No impurity peak was observed in XRD patterns of Al_2O_3-modified samples and Al_2O_3-coated sample although Al^{3+} might diffuse into

the crystal lattice of Al_2O_3-modified $Li(Ni_{1/3}Co_{1/3}Mn_{1/3})O_2$ during synthesis. The lattice constants of all samples were calculated by PowderX software. Table 2 shows lattice constants and the intensity ratio of (003) peak and (104) peak ($I_{(003)}/I_{(104)}$). The

Table 2
Cell parameters and the value of $I_{(003)}/I_{(104)}$ of bare, Al_2O_3-modified and Al_2O_3-coated $Li(Ni_{1/3}Co_{1/3}Mn_{1/3})O_2$.

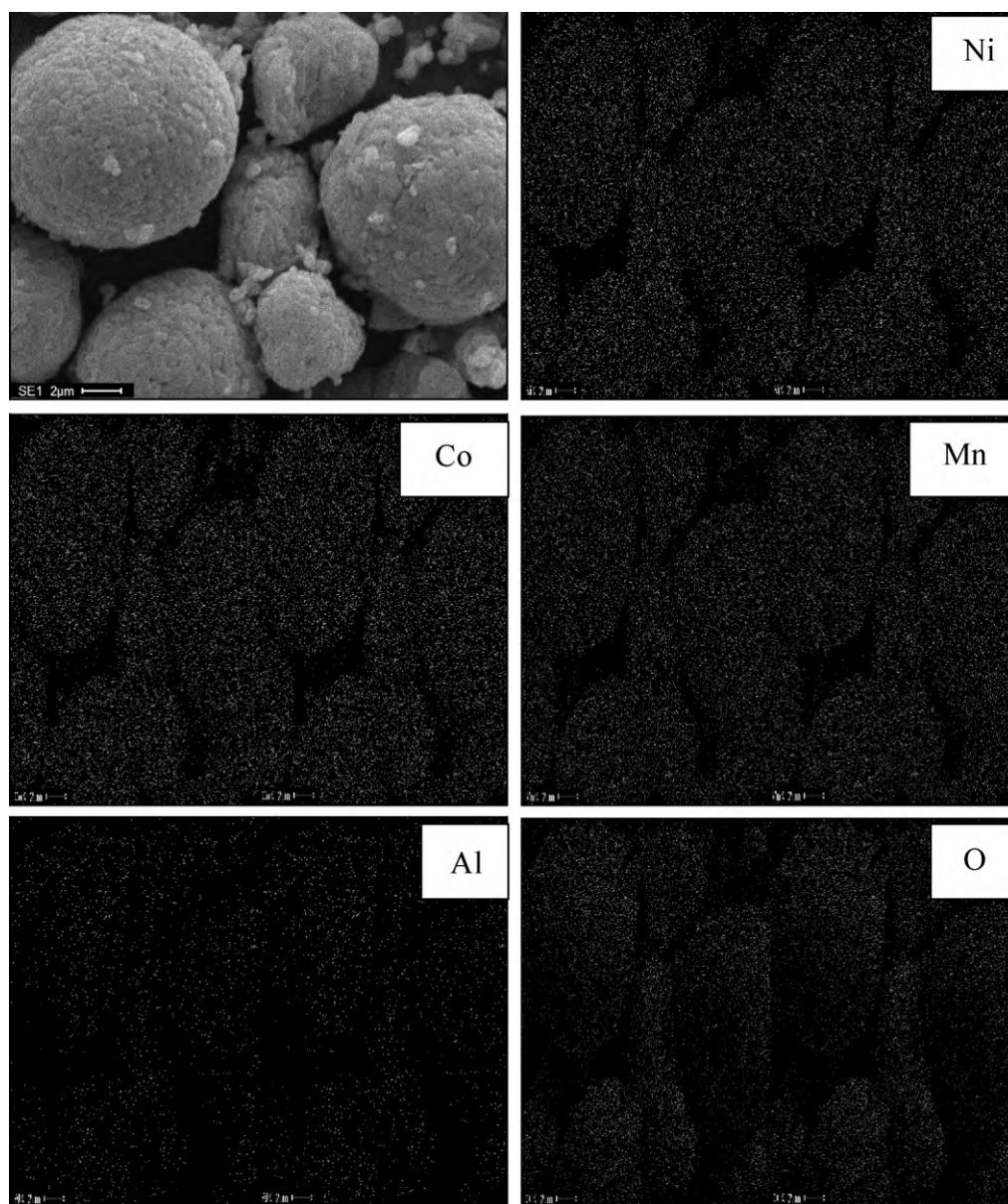| Sample	Lattice constant a (nm)	Lattice constant c (nm)	$I_{(003)}/I_{(104)}$
Bare	0.28603	1.42305	1.66
0.5% Al_2O_3-modified	0.28602	1.42304	1.87
1% Al_2O_3-modified	0.28599	1.42289	1.90
2% Al_2O_3-modified	0.28592	1.42247	1.57
5% Al_2O_3-modified	0.28580	1.42202	1.52
1% Al_2O_3-coated	0.28603	1.42291	1.68

Fig. 2. EDS mapping patterns of 1% Al_2O_3-modified $Li(Ni_{1/3}Co_{1/3}Mn_{1/3})O_2$.
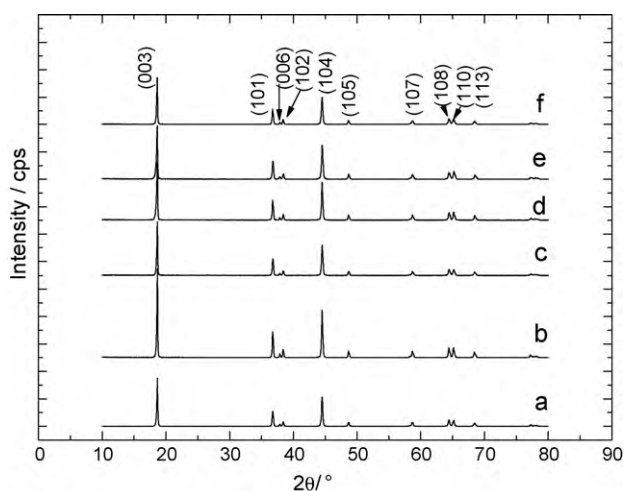

Fig. 3. XRD patterns of bare (a), 0.5% (b), 1% (c), 2% (d), 5% (e) Al_2O_3-modified $Li(Ni_{1/3}Co_{1/3}Mn_{1/3})O_2$ and 1% Al_2O_3-coated $Li(Ni_{1/3}Co_{1/3}Mn_{1/3})O_2$ (f).

intensity ratio of $I_{(003)}/I_{(104)}$ has been reported to be strongly correlated to undesirable cation mixing of $Li(Ni_{1/3}Co_{1/3}Mn_{1/3})O_2$ [17]. As far as Al_2O_3-modified samples were concerned, the lattice constants a and c showed a gradual decrease with increasing Al content. Nevertheless, the value of $I_{(003)}/I_{(104)}$ first increased and then decreased with increasing Al content. The variety of lattice constants and $I_{(003)}/I_{(104)}$ indicate that Al might incorporate into the lattice crystal of Al_2O_3-modified $Li(Ni_{1/3}Co_{1/3}Mn_{1/3})O_2$. Because the ion radius of Al^{3+} (0.0535 nm) is close to that of Co^{3+} (0.0545 nm) and Mn^{4+} (0.053 nm) the effect of Al^{3+} incorporation on lattice constants is inconsiderable [18,19]. However, the effect of Al_2O_3 modification on $I_{(003)}/I_{(104)}$ is very obvious. As shown in Table 2, 1% Al_2O_3-modified $Li(Ni_{1/3}Co_{1/3}Mn_{1/3})O_2$ shows the largest value of $I_{(003)}/I_{(104)}$. This means that 1% Al_2O_3-modified $Li(Ni_{1/3}Co_{1/3}Mn_{1/3})O_2$ has the best stability of structure. On the contrary, the lattice constants and $I_{(003)}/I_{(104)}$ of 1% Al_2O_3-coated $Li(Ni_{1/3}Co_{1/3}Mn_{1/3})O_2$ was same with that of bare sample. So, traditional Al_2O_3 coating process do not affect the structure of $Li(Ni_{1/3}Co_{1/3}Mn_{1/3})O_2$.
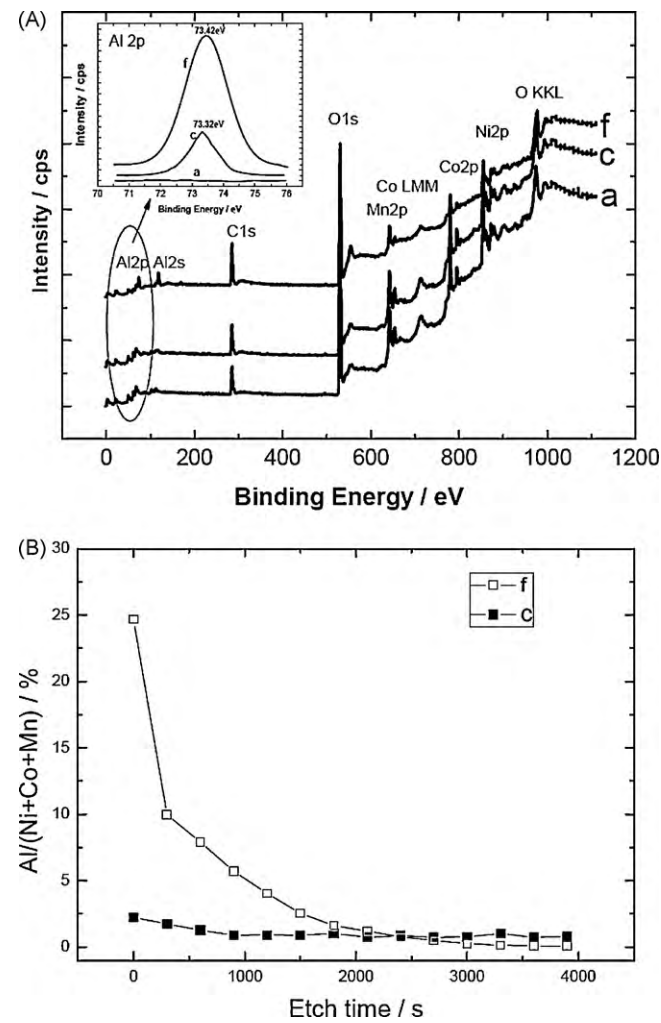
Fig. 4. (A) XPS patterns of bare (a), 1% Al_2O_3-modified $Li(Ni_{1/3}Co_{1/3}Mn_{1/3})O_2$ (c) and 1% Al_2O_3-coated $Li(Ni_{1/3}Co_{1/3}Mn_{1/3})O_2$ (f). Inset graph is magnified XPS spectra of Al2p. (B) Depth Al element distribution profiles of 1% Al_2O_3-modified $Li(Ni_{1/3}Co_{1/3}Mn_{1/3})O_2$ (c) and 1% Al_2O_3-coated $Li(Ni_{1/3}Co_{1/3}Mn_{1/3})O_2$ (f).

3.3. Analysis of the surface of Al_2O_3-modified $Li(Ni_{1/3}Co_{1/3}Mn_{1/3})O_2$ by XPS

XPS was employed to examine the valence and the radial distribution of Al and transition metal elements in Al_2O_3-coated and Al_2O_3-modified $Li(Ni_{1/3}Co_{1/3}Mn_{1/3})O_2$. Fig. 4(a) shows XPS patterns of bare, 1% Al_2O_3-modified and 1% Al_2O_3-coated $Li(Ni_{1/3}Co_{1/3}Mn_{1/3})O_2$. In all samples, the binding energies of electrons in Ni 2p3/2, Co2p3/2 and Mn 2p3/2 are 854.5 eV, 779.9 eV and 642.3 eV, respectively, in good agreement with Ref. [11]. The result indicates that the dominant valences of Ni, Co, and Mn are divalent, trivalent and tetravalent, respectively. The XPS spectra

of Al 2p were found in 1% Al_2O_3-modified sample and 1% Al_2O_3-coated sample and the binding energies of electrons in Al 2p are both 73.3 eV. The result indicates that valence of Al is trivalent [20]. The inset graph of Fig. 4(a) shows the enlarged XPS patterns of Al 2p. Although Al content is same, the intensity of Al 2p peak of Al_2O_3-coated sample was much higher than that of Al_2O_3-modified sample. The result supports the fact that the Al concentration on the surface of Al_2O_3-coated sample is much higher than that of Al_2O_3-modified sample. Fig. 4(b) demonstrates the dependence of Al/(Ni + Co + Mn) vary on the etching time. As for 1% Al_2O_3-coated sample, the ratio of Al/(Ni + Co + Mn) decreased gradually from 24.7% to 0% with increasing etching time. The result indicates that the Al of Al_2O_3-coated sample exist only on the surface of particles. The high Al concentration on the surface may lead to a dense Al_2O_3 coating layer, which is adverse to Li^+ transport and charge transfer. The Al distribution of Al_2O_3-modified sample showed large difference with that of Al_2O_3-coated sample prepared by traditional process. The initial value of Al/(Ni + Co + Mn) was about 2.2%, which was much lower than that of Al_2O_3-coated sample. The ratio of Al/(Ni + Co + Mn) decreased gradually first with increasing etching. When the etching time was over 900 s, the ratio of Al/(Ni + Co + Mn) tended to keep stable. The result shows that only a little Al exist on the surface of Al_2O_3-modified sample as a thin coating layer and most of Al diffuse into the bulk of Al_2O_3-modified $Li(Ni_{1/3}Co_{1/3}Mn_{1/3})O_2$ and affect the structure of $Li(Ni_{1/3}Co_{1/3}Mn_{1/3})O_2$.

3.4. Electrochemical properties of Al_2O_3-modified $Li(Ni_{1/3}Co_{1/3}Mn_{1/3})O_2$

2032 coin cell was employed to study the effect of Al_2O_3 modification on electrochemical performance. All cells were charged and discharged at 0.2 C current in the voltage ranges of 4.3–3.0 V and 4.5–3.0 V, respectively. The charging and discharging curves (not shown) of all cells were quite smooth, and the discharging average voltage did not change noticeably after Al_2O_3 modification or coating. The initial charge and discharge capacity of all samples are shown in Table 3. The discharge capacity of bare $Li(Ni_{1/3}Co_{1/3}Mn_{1/3})O_2$ was 149 mAh g^{-1} at 4.3–3.0 V. When the charge cut-off voltage increased to 4.5 V, the discharge capacity increased to 171.1 mAh g^{-1}. In terms of Al_2O_3-modified samples, when the ratio of Al/(Ni + Co + Mn) is 0.5%, 1% and 2%, the discharge capacity were 151.8 mAh g^{-1}, 152.5 mAh g^{-1} and 150 mAh g^{-1}, respectively at 4.3–3.0 V. The result shows that when Al/(Ni + Co + Mn) ≤ 2% the reversible capacity of Al_2O_3-modified $Li(Ni_{1/3}Co_{1/3}Mn_{1/3})O_2$ do not decrease because of Al_2O_3 modification. On the contrary, 1% Al_2O_3-coated $Li(Ni_{1/3}Co_{1/3}Mn_{1/3})O_2$ delivered a reversible capacity of 145.8 mAh g^{-1}. Obvious loss of capacity is caused by Al_2O_3 coating. Although 5% Al_2O_3-modified $Li(Ni_{1/3}Co_{1/3}Mn_{1/3})O_2$ also shows perceptible capacity loss, the capacity loss can be ascribed to the decrease of active material amount caused by high Al content.

Cycle performance of all samples was examined in the voltage ranges of 4.3–3.0 V and 4.5–3.0 V at 0.5 C current charging

Table 3
Charge capacity, discharge capacity and irreversible capacity of all samples in the first cycle (capacity unit: mAh g^{-1}).

Sample	4.3–3.0 V			4.5–3.0 V		
	Charge capacity	Discharge capacity	Irreversible capacity	Charge capacity	Discharge capacity	Irreversible capacity
Bare	169.8	149.2	20.6	196.4	171.1	25.3
0.5% Al_2O_3-modified	172.5	151.8	20.7	198.0	173.6	24.4
1% Al_2O_3-modified	170.2	152.5	17.7	199.0	173.5	25.5
2% Al_2O_3-modified	170.4	150.0	20.4	196.8	172.9	23.9
5% Al_2O_3-modified	164.7	143.8	20.9	194.9	167.1	27.8
1% Al_2O_3-coated	165.6	145.8	19.8	202.6	166.4	36.2

Y. Huang et al. / Journal of Power Sources 195 (2010) 8267–8274
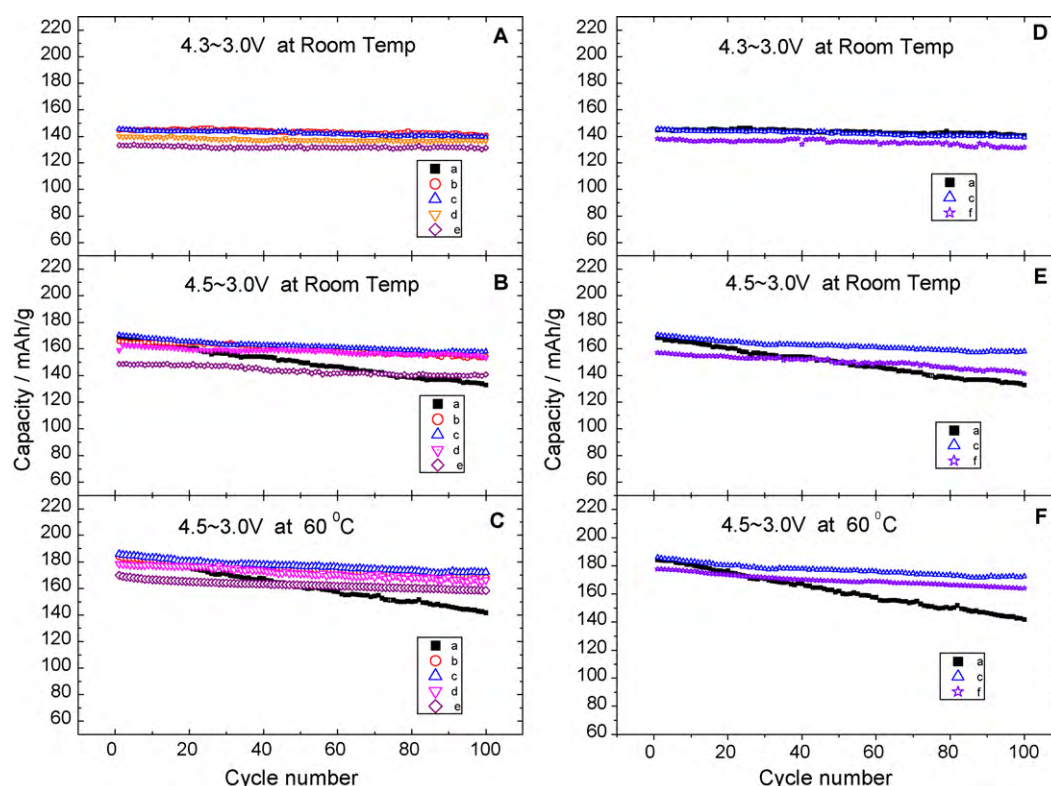
Fig. 5. Cycle performance of bare, Al_2O_3-modified and Al_2O_3-coated $Li(Ni_{1/3}Co_{1/3}Mn_{1/3})O_2$. Left graphs (A–C) show the effect of Al content of Al_2O_3-modified samples on cycle performance at different experiment condition. Right graphs (D–F) show the effect of Al_2O_3 modification and Al_2O_3 coating on cycle performance at different experiment condition. (a–f) represent bare sample, 0.5%, 1%, 2%, 5% Al_2O_3-modified sample and 1% Al_2O_3-coated sample, respectively. Experiment condition: 0.5 C charge and discharge, 4.3–3.0 V at room temperature (A and D), 4.5–3.0 V at room temperature (B and E) and 4.5–3.0 V at 60 °C (C and F).

and discharging. As shown in Fig. 5, all samples exhibit good cycle performance under 4.3–3.0 V at room temperature. When the charge cut-off voltage increased to 4.5 V, reversible capacity of bare $Li(Ni_{1/3}Co_{1/3}Mn_{1/3})O_2$ faded from 168.4 mAh g^{-1} to 132.7 mAh g^{-1} during 100 cycles and the capacity retention rate was only 78.8%. In contrast, both Al_2O_3-modified samples and Al_2O_3-coated sample showed good cycle performance at 4.5–3.0 V. The discharge capacity of 1% Al_2O_3-modified sample reduced from 170.6 mAh g^{-1} to 158.6 mAh g^{-1} after 100 cycles and the capacity retention rate reached 93%. As far as 1% Al_2O_3-coated sample was concerned, the discharge capacity reduced from 156.9 mAh g^{-1} to 141.1 mAh g^{-1} and the capacity retention rate was 90%. Therefore, the cycle performance of $Li(Ni_{1/3}Co_{1/3}Mn_{1/3})O_2$ under high charge cut-off voltage can be improved significantly by Al_2O_3 modification and Al_2O_3 coating. However, 1% Al_2O_3-modified $Li(Ni_{1/3}Co_{1/3}Mn_{1/3})O_2$ delivers higher capacity and shows better capacity retention than 1% Al_2O_3-coated sample. As shown in Fig. 5(c) and (f), the similar result is also observed in cycle performance measurement at 4.5–3.0 V and 60 °C.

In order to investigate the effect of Al_2O_3 coating and Al_2O_3 modification on rate capability of $Li(Ni_{1/3}Co_{1/3}Mn_{1/3})O_2$, the cells were first charged to 4.3 V at 0.2 C and then discharged to 3.0 V at currents of 0.2 C, 1 C, 5 C, 10 C, 20 C and 40 C, respectively. The capacity retention rate at different discharged current is shown in Fig. 6(a). It is clear that Al_2O_3 coating cause rate capability worse but Al_2O_3 modification can enhance the rate capability of $Li(Ni_{1/3}Co_{1/3}Mn_{1/3})O_2$. As shown in Fig. 6, 1% Al_2O_3-modified $Li(Ni_{1/3}Co_{1/3}Mn_{1/3})O_2$ shows better retention of capacity and discharging platform than 1% Al_2O_3-coated sample when discharging current increase gradually. So, compared with 1% Al_2O_3-coated sample, 1% Al_2O_3-modified $Li(Ni_{1/3}Co_{1/3}Mn_{1/3})O_2$ shows better rate capability.

According to former report [8], the structure of $Li(Ni_{1/3}Co_{1/3}Mn_{1/3})O_2$ is still stable when it is charged to 4.5 V. So, capacity fade of $Li(Ni_{1/3}Co_{1/3}Mn_{1/3})O_2$ at high charge cut-off voltage is mainly ascribed to side reaction on the interphase between electrode and electrolyte [9,21]. Surface coating and modification are good methods to enhance stability of interphase between electrode and electrolyte [11–16]. As XPS and SEM show, a relative thick Al_2O_3 coating layer exists on the surface of 1% Al_2O_3-coated $Li(Ni_{1/3}Co_{1/3}Mn_{1/3})O_2$. The thick inert Al_2O_3 coating layer can enhance stability of interphase between electrode and electrolyte. Nevertheless, the thick inert Al_2O_3 coating layer shows poor electronic and ionic conductivity, and moreover, it might hinder Li^+ intercalation and deintercalation during charging/discharging process. Therefore, 1% Al_2O_3-modified $Li(Ni_{1/3}Co_{1/3}Mn_{1/3})O_2$ shows better cycle performance but lower capacity and worse rate capability than bare sample. As for 1% Al_2O_3-modified $Li(Ni_{1/3}Co_{1/3}Mn_{1/3})O_2$, Li^+ diffuse into the bulk of $(Ni_{1/3}Co_{1/3}Mn_{1/3})(OH)_2$ through Al_2O_3 coating layer and Al^{3+} can also diffuse into the bulk from surface during synthesis process. As XPS result shows, only a little Al exist on the surface of 1% Al_2O_3-modified $Li(Ni_{1/3}Co_{1/3}Mn_{1/3})O_2$ as a thin coating layer and most of Al diffuse into the crystal lattice of $Li(Ni_{1/3}Co_{1/3}Mn_{1/3})O_2$. So, the surface coating layer of 1% Al_2O_3-modified sample is thinner than that of 1% Al_2O_3-coated sample, meanwhile, it can supply Li^+ diffused tunnel during charging/discharging process. The thin special coating layer not only can stabilize the interphase of electrode/electrolyte but also shows better Li^+ conductivity than inert Al_2O_3 coating layer. Furthermore, the Al^{3+} entering crystal lattice of $Li(Ni_{1/3}Co_{1/3}Mn_{1/3})O_2$ is helpful to stabilize the structure and enhance rate capability during charging and discharging process [22–24]. Consequently, 1% Al_2O_3-modified $Li(Ni_{1/3}Co_{1/3}Mn_{1/3})O_2$ not only show improved cycle performance
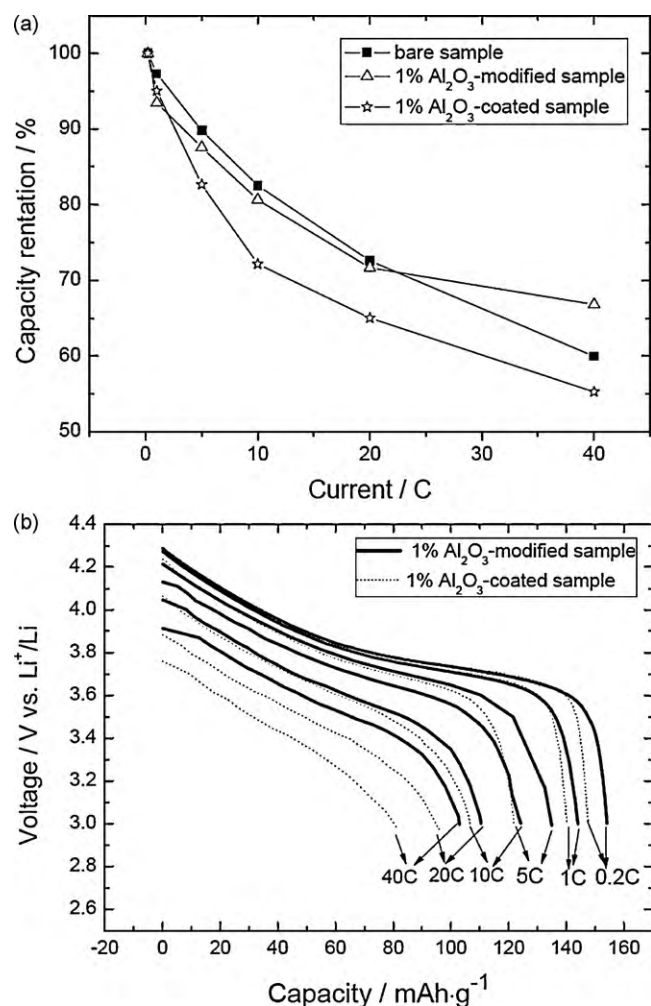
Fig. 6. Rate capability of bare, 1% Al$_2$O$_3$-modified sample and 1% Al$_2$O$_3$-coated sample. (a) Capacity retention rate at different current. (b) Discharge curves at different current.

without capacity loss but also enhance the rate capability of Li(Ni$_{1/3}$Co$_{1/3}$Mn$_{1/3}$)O$_2$.

So as to understand the improvement in the electrochemical properties caused by Al$_2$O$_3$ modification, the kinetics parameters of Li$^+$ intercalation/deintercalation reaction were measured via electrochemical impedance spectroscopy (EIS) experiments. Fig. 7 shows the Nyquist plots of all samples measured at 4.5 V vs. Li$^+$/Li and corresponding equivalent circuit (inset graph). In Fig. 7, the intercept at Z axis in high frequency refers to inner resistance of cell (R_s); the semi-circle in the high frequency range is caused by surface film resistance and charge transfer resistance on the interface of Li/electrolyte (R_f) [25]; the semi-circle in the middle frequency range reflects the charge transfer resistance on the interface of cathode/electrolyte (R_{ct}); the sloping line in the lower frequency represents Warburg impedance (W), which is related to lithium-ion diffusion in solid phase. The value of R_{ct} was obtained by applying Zview software to simulate EIS data. As shown in Table 4, very small increase of R_{ct} is caused by 1% Al$_2$O$_3$ modification but 1% Al$_2$O$_3$ coating leads to evident increase of R_{ct}.

In the linear part of EIS, which is directly related to Li$^+$ diffusion in material bulk, the relation between imaginary resistance (Z') and frequency (ω) fit the following equation [16].
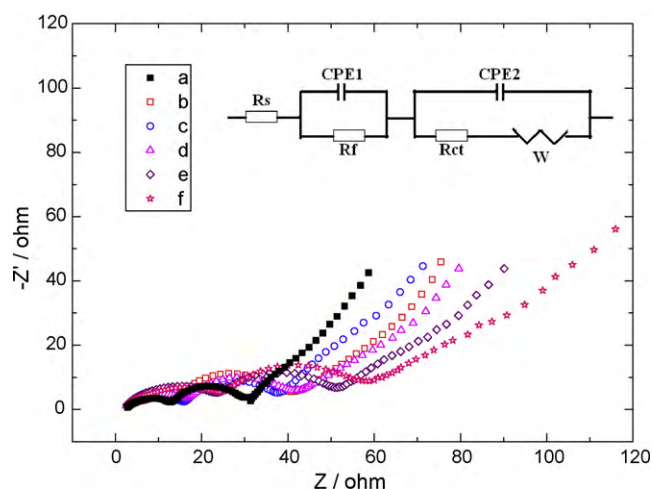
$$Z' = K - A_w \omega^{-1/2} \tag{1}$$

Fig. 7. Electrochemical impedance spectra of bare (a), 0.5% (b), 1% (c), 2% (d), 5% (e) Al$_2$O$_3$-modified Li(Ni$_{1/3}$Co$_{1/3}$Mn$_{1/3}$)O$_2$ and 1% Al$_2$O$_3$-coated Li(Ni$_{1/3}$Co$_{1/3}$Mn$_{1/3}$)O$_2$ (f). The inset graph is corresponding equivalent circuit. R_s: solution resistance; R_f: surface film resistance; R_{ct}: charge transfer resistance; W: Warburg impedance. CPE1 and CPE2 are constant phase angle element.

In Eq. (1), K is a constant and A_w is the Warburg coefficient. From the plot of Z' as a function of $\omega^{-1/2}$ (not shown), the slope A_w can be obtained. Based on the following equation [26], Li$^+$ diffused coefficient (D_{Li}) can be calculated.

$$D_{Li} = \frac{1}{2}\left[\left(\frac{V_m}{FAA_w}\right)\frac{dE}{dx}\right]^2 \tag{2}$$

In Eq. (2), V_m is the molar volume; F is the Faraday constant; A is the electrode area. The dE/dx can be obtained from the galvanostatic titration curve (not shown). D_{Li} of all samples were calculated. As shown in Table 4, D_{Li} of Al$_2$O$_3$-modified samples increase first and then decreases with increasing Al content. 1% Al$_2$O$_3$-modified sample showed the highest value of D_{Li} (8.48×10^{-9} cm^2 s^{-1}), which was larger than that of bare sample (7.12×10^{-9} cm^2 s^{-1}). On the contrary, 1% Al$_2$O$_3$-coated sample showed a lower value of D_{Li} (4.58×10^{-9} cm^2 s^{-1}) than that of bare sample. The result proves that the Al$_2$O$_3$ modification can speed up Li$^+$ diffusion of Li(Ni$_{1/3}$Co$_{1/3}$Mn$_{1/3}$)O$_2$ but traditional Al$_2$O$_3$ coating method decelerate it.

In order to study the effect of Al$_2$O$_3$ modification on interfacial lithium-ion transfer process of Li(Ni$_{1/3}$Co$_{1/3}$Mn$_{1/3}$)O$_2$, temperature dependence of the interfacial lithium-ion transfer resistances (R_{ct}) was measured. The following equation [27] shows the connection of temperature, R_{ct} and activation energy (E_a) of the charge transfer reaction.

$$\lg\frac{T}{R_{ct}} = \lg A - \frac{E_a}{2.303R} \times \frac{1}{T} \tag{3}$$

Here E_a is the activation energy; T is the absolute temperature; R is the gas constant; R_{ct} is the charge transfer resistance; A is the pre-exponential factor. Fig. 8 shows the plot of $\lg(T/R_{ct})$ as a function of 1000/T. The activation energies were calculated from slope of

Table 4
Charge transfer resistance (R_{ct}), Li$^+$ diffusion coefficient (D_{Li}) and activation energy (E_a) of bare, Al$_2$O$_3$-modified and Al$_2$O$_3$-coated Li(Ni$_{1/3}$Co$_{1/3}$Mn$_{1/3}$)O$_2$.

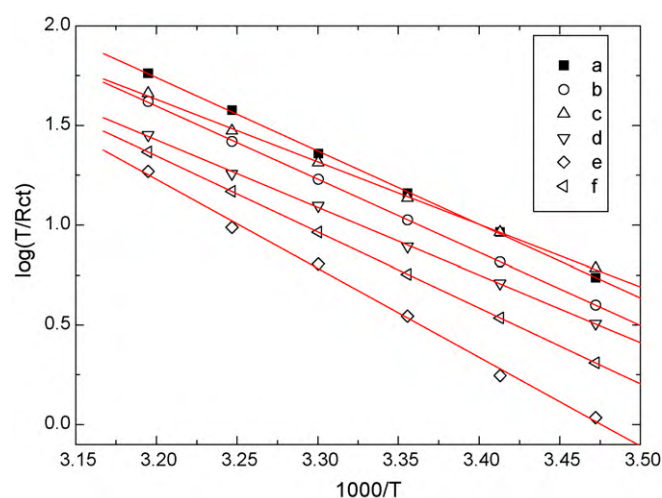| Sample	R_{ct} (ohm)	D_{Li} (cm^2 s^{-1})	E_a (kJ mol^{-1})
Bare	20.6	7.12×10^{-9}	70.5
0.5% Al$_2$O$_3$-modified	22.5	7.44×10^{-9}	69.0
1% Al$_2$O$_3$-modified	22.7	8.48×10^{-9}	60.1
2% Al$_2$O$_3$-modified	21.5	8.18×10^{-9}	64.9
5% Al$_2$O$_3$-modified	24.2	6.48×10^{-9}	72.9
1% Al$_2$O$_3$-coated	30.4	4.58×10^{-9}	85.4

Fig. 8. Temperature dependency for interfacial lithium-ion transfer resistance of bare (a), 0.5% (b), 1% (c), 2% (d), 5% (e) Al_2O_3-modified $Li(Ni_{1/3}Co_{1/3}Mn_{1/3})O_2$ and 1% Al_2O_3-coated $Li(Ni_{1/3}Co_{1/3}Mn_{1/3})O_2$ (f) in $1.0\,mol\,L^{-1}$ $LiPF_6/(EC:EMC:DEC = 1:1:1)$.

plots. As shown in Table 4, E_a of bare sample is $70.5\,kJ\,mol^{-1}$, which is close to the result of our former report [16]. E_a of Al_2O_3-modified samples increased first and then decreased with increasing Al content. 1% Al_2O_3-modified $Li(Ni_{1/3}Co_{1/3}Mn_{1/3})O_2$ showed the lowest value of E_a ($60.1\,kJ\,mol^{-1}$), which was lower than that of bare sample. In contrast, E_a of 1% Al_2O_3-coated $Li(Ni_{1/3}Co_{1/3}Mn_{1/3})O_2$ was $85.4\,kJ\,mol^{-1}$, which was higher than that of bare sample. The activation energy change can be caused by following reason: (1) change of side reactions occur on the interface of electrode/electrolyte; (2) change of lithium-ion transfer mechanism [28]. In our former report, ZrO_2 modification could decrease the activation energy but the effect was smaller than Al_2O_3 modification [16]. If the decrease of activation energy was only due to the prevention of some side reactions, the activation energy will obtain a same value in both cases and be independent of modification oxides. Therefore, we deduce that the decrease of activation energy of Al_2O_3-modified sample mostly caused by the change of lithium-ion transfer mechanism, which is associated with interactions between modification oxides and Li^+. Although precise mechanism cannot still be clarified in this paper, it is clear that Al_2O_3 modification can speed up the interfacial lithium-ion transfer process but Al_2O_3 coating might hinder the process.

4. Conclusion

In this paper, a modified Al_2O_3 coating process was introduced to enhance the electrochemical performance of $Li(Ni_{1/3}Co_{1/3}Mn_{1/3})O_2$. Al_2O_3-modified $Li(Ni_{1/3}Co_{1/3}Mn_{1/3})O_2$ with different Al content and 1% Al_2O_3-coated $Li(Ni_{1/3}Co_{1/3}Mn_{1/3})O_2$ were synthesized by the modified Al_2O_3 coating process and traditional Al_2O_3 coating process, respectively. The effects of the Al_2O_3 modification and traditional Al_2O_3 coating on structure and electrochemical performance have been investigated and compared. XPS and XRD results indicate that only a little Al covers the surface of Al_2O_3-modified $Li(Ni_{1/3}Co_{1/3}Mn_{1/3})O_2$ as a thin Al_2O_3 coating layer and most Al diffuses into the crystal lattice of Al_2O_3-modified $Li(Ni_{1/3}Co_{1/3}Mn_{1/3})O_2$. As for Al_2O_3-coated sample, the Al only exist the surface of particle as a thick inert Al_2O_3 coating layer. Electrochemical performance tests show that 1% Al_2O_3 modification can enhance the cycle performance and rate capability without capacity loss but 1% Al_2O_3 coating lead to evident capacity loss and decline of rate capability. The difference of electrochemical performance may be correlated to Al element distribution of Al_2O_3-coated and Al_2O_3-modified sample. EIS results prove that the Al_2O_3 modification can speed up Li^+ diffusion of $Li(Ni_{1/3}Co_{1/3}Mn_{1/3})O_2$ and decrease activation energy of charge transfer reaction but traditional Al_2O_3 coating method cause adverse function. Therefore, compared with traditional Al_2O_3 coating process, the modified Al_2O_3 coating process is a better choice to enhance electrochemical performance of $Li(Ni_{1/3}Co_{1/3}Mn_{1/3})O_2$.

Acknowledgement

References

[1] J.B. Goodenough, J. Power Sources 174 (2007) 996–1000.
[2] M. Armand, J.-M. Tarascon, Nature 451 (2008) 652–657.
[3] K. Kang, Y.S. Meng, J. Breǐger, C.P. Grey, G. Ceder, Science 311 (2006) 977–980.
[4] M.S. Whittingham, Chem. Rev. 104 (2004) 4271–4301.
[5] Y.-K. Sun, S.-T. Myung, B.-C. Park, J. Prakash, I. Belharouak, K. Amine, Nat. Mater. 8 (2009) 1–5.
[6] J.W. Fergus, J. Power Sources 195 (2010) 939–954.
[7] T. Ohzuku, Y. Makimura, Chem. Lett. 7 (2001) 642–643.
[8] N. Yabuuchi, T. Ohzuku, J. Power Sources 119–121 (2003) 171–174.
[9] K.M. Shaju, G.V.S. Rao, B.V.R. Chowdari, Electrochim. Acta 48 (2002) 145–151.
[10] G.-H. Kim, M.-H. Kim, S.-T. Myung, Y.K. Sun, J. Power Sources 146 (2005) 602–605.
[11] D. Li, Y. Kato, K. Kobayakawa, H. Noguchi, Y. Sato, J. Power Sources 160 (2006) 1342–1348.
[12] Y. Kim, H.S. Kim, S.W. Martin, Electrochim. Acta 52 (2006) 1316–1322.
[13] S.-K. Hu, G.-H. Cheng, M.-Y. Cheng, B.-J. Hwang, J. Power Sources 188 (2009) 564–569.
[14] H. Cao, B. Xia, Y. Zhang, N. Xu, Solid State Ionics 176 (2005) 911–914.
[15] H.-S. Kim, Y. Kim, S.-I. Kim, S.W. Martin, J. Power Sources 161 (2006) 623–627.
[16] Y. Huang, J. Chen, J. Ni, H. Zhou, X. Zhang, J. Power Sources 188 (2009) 538–545.
[17] D.D. MacNeil, Z.H. Lu, J.R. Dahn, J. Electrochem. Soc. 149 (2002) A1332–A1336.
[18] R.D. Shannon, Acta Crystallogr. A 32 (1976) 751–767.
[19] T. Ohzuku, A. Ueda, M. Nagayama, J. Electrochem. Soc. 140 (1993) 1862–1870.
[20] L. Dussault, J.C. Dupin, C. Guimon, M. Monthioux, N. Latorre, T. Ubieto, E. Romeo, C. Royo, A. Monzón, J. Catal. 251 (2007) 223–232.
[21] S.-T. Myung, K. Izumi, S. Komaba, Y.-K. Sun, H. Yashiro, N. Kumagai, Chem. Mater. 17 (2005) 3695–3704.
[22] B. Zhang, G. Chen, Y. Liang, P. Xu, Solid State Ionics 180 (2009) 398–404.
[23] S.-K. Hu, T.-C. Chou, B.-J. Hwang, G. Ceder, J. Power Sources 160 (2006) 1287–1293.
[24] Y.-K. Lin, C.-H. Lu, J. Power Sources 189 (2009) 353–358.
[25] T. Abe, M. Ohtsuka, F. Sagane, Y. Iriyama, Z. Ogumi, J. Electrochem. Soc. 151 (2004) A1950–A1953.
[26] K.M. Shaju, G.V.S. Rao, B.V.R. Chowdari, J. Electrochem. Soc. 151 (2004) A1324–A1332.
[27] N. Nakayama, T. Nozawa, Y. Iriyama, T. Abe, Z. Ogumi, K. Kikuchi, J. Power Sources 174 (2007) 695–700.
[28] Y. Iriyama, H. Kurita, I. Yamada, T. Abe, Z. Ogumi, J. Power Sources 137 (2004) 111–116.